

# Design and Fabrication of RF MEMS Switch by the CMOS Process

Ching-Liang Dai<sup>1\*</sup>, Hsuan-Jung Peng<sup>1</sup>, Mao-Chen Liu<sup>1</sup>, Chyan-Chyi Wu<sup>2</sup>  
and Lung-Jieh Yang<sup>3</sup>

<sup>1</sup>*Department of Mechanical Engineering, National Chung Hsing University  
Taichung, Taiwan 402, R.O.C.*

<sup>2</sup>*Center for Measurement standards, Industrial Technology Research Institute,  
Hsinchu, Taiwan 300, R.O.C.*

<sup>3</sup>*Department of Mechanical and Electro-Mechanical Engineering, Tamkang University  
Tamsui, Taiwan 251, R.O.C.*

## Abstract

This work investigates the fabrication of a RF (ratio frequency) MEMS (micro elector mechanical system) switch using the standard 0.35  $\mu\text{m}$  2P4M (double polysilicon four metal) CMOS (complementary metal oxide semiconductor) process and the post-process. The switch is a capacitive type, which is actuated by an electrostatic force. The structure of the switch consists of a CPW (coplanar waveguides) transmission lines and a suspended membrane. The CPW lines and the membrane are the metal layers of the CMOS process. The main advantage of the RF switch is only needed a simple post-process, which is compatible with the CMOS process. The post-process uses an etchant, silox vapox III, to etch oxide layer to release the suspended membrane and springs. Experiment results show that the pull-in voltage of the switch is about 17 V. The insertion loss and return loss in the range of 10 to 40 GHz are  $-2.5$  dB and  $-13$  dB, respectively.

**Key Words:** CMOS, Post-process, MEMS, RF Switch

## 1. Introduction

Microelectronic switches, such as GaAs MESFETs (metal-semiconductor field effect transistor) and PIN (positive-intrinsic-negative) diode switches, are commonly used in the RF communication. The disadvantages of microelectronic switches are high insertion loss and bad isolation in the 'on/off' switching state. Unlike these microelectronic switches, the RF switches fabricated by MEMS technology have low insertion loss and good isolation at microwave and millimeter wave frequencies [1]. Theoretically, micromachined RF switches do not exhibit inter-modulation distortion (IMD) owing

that there is no I–V nonlinearity [2]. The main limitation of MEMS switches is high driving voltage.

Micromechanical microwave switches were first demonstrated in 1971 using bulk-micromachined cantilever switches [3]. Since then, many different types of shunt capacitive MEMS switches have been reported [4–8]. These switches were fabricated on the GaAs substrate or high-resistivity to reduce the substrate loss. A micromachined microwave transmission lines fabricated by the CMOS technology was presented [9]. The transmission line was designed to operate in TEM (transverse-electric-magnetic) mode, with  $50\text{-}\Omega$  nominal characteristic impedance.

The advantage of micromachined devices fabricated by the CMOS-MEMS technique is compatible with the

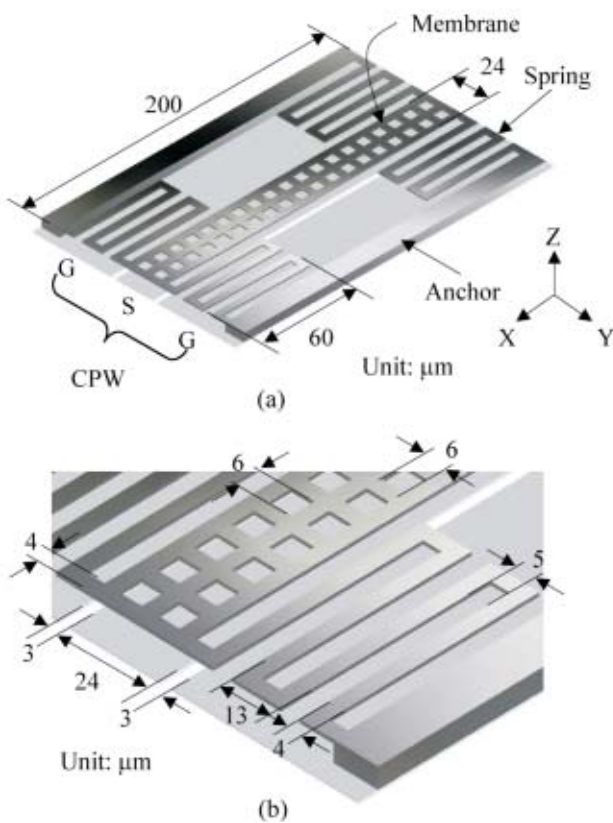
---

\*Corresponding author. E-mail: cldai@dragon.nchu.edu.tw

CMOS process, and thus the devices can easily integrate with integration circuits on chip [10]. This study utilizes the CMOS-MEMS technique to fabricate a RF switch. The main benefit of the RF switch is only needed a simple post-process, which is compatible with the CMOS process. The post-process uses a silox vapox III etchant to etch oxide layer to release the suspended structures. The switch is a capacitive type, which is actuated by an electrostatic force. The switch structures contain a CPW transmission lines, a membrane, springs and anchors. The membrane, springs, anchors and CPW lines are the metal layers of the CMOS process. Experiment results show that the pull-in voltage of the switch is about 17 V. The insertion loss and return loss in the range of 10 to 40 GHz are -2.5 dB and -13 dB, respectively.

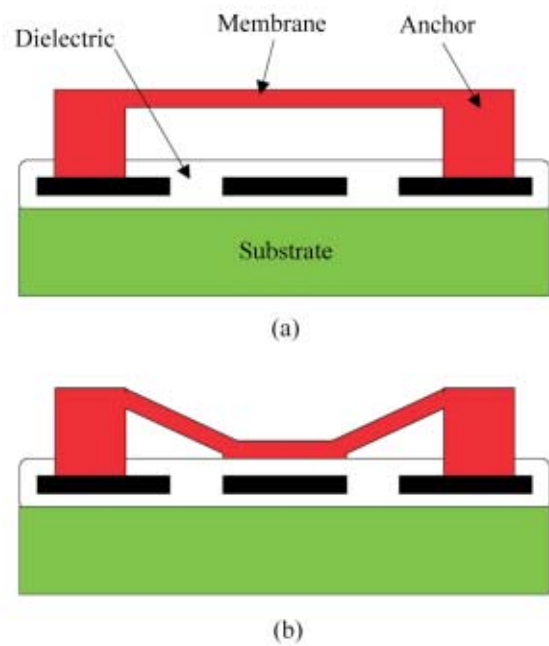
### 2. Design of Switch Structures

Figure 1(a) illustrates the structures of the RF switch. The switch contains a CPW transmission lines and a



**Figure 1.** Structure and dimensions of a RF switch: (a) CPW transmission lines and suspended membrane; (b) flexural supported springs.

membrane, springs and anchors. The CPW transmission lines consists of three lines, which are ground (G), signal (S) and ground (G) lines. The membrane over the signal line of CPW is supported by four S-shape springs. All springs are anchored on the ground lines of CPW. Material of the membrane, springs, anchors and CPW lines is aluminum metal. Figure 1(b) shows the dimensions of the RF switch. The area of the membrane is  $200 \times 24 \mu\text{m}^2$ . The width of the signal line of CPW is  $24 \mu\text{m}$ . The gap between the signal line and the ground line of CPW is  $3 \mu\text{m}$ . The width of all springs is  $4 \mu\text{m}$ . The thickness of the membrane, springs and CPW lines is approximately  $1 \mu\text{m}$ . The gap between the membrane and the signal line is about  $3.5 \mu\text{m}$ . Figure 2 depicts the cross-section view of RF switch. The switch is a capacitive type that is actuated by the electrostatic force. Figure 2(a) shows that the switch is ‘on’ state when without the applied voltage. The membrane supported by the stiffness of springs stays in the up position, and the RF signal can propagate by the signal line of CPW. Figure 2(b) demonstrates that the switch is ‘off’ state when with the applied voltage. The membrane actuated by the electrostatic force locates in the down position when the driving voltage applies to the signal and ground lines of CPW. The



**Figure 2.** Schematic of cross-section view of RF switch: (a) in the unactuated state or ‘on’ state; (b) in the actuated state or ‘off’ state.

RF signal in the signal line of CPW is coupled to the ground lines owing that a high capacitance generated between the membrane and the signal line of CPW. The geometry of the CPW structure affects its characteristic impedance and propagation constant in the desired quasi-TEM mode of operation. The CPW is designed to operate in TEM mode, with 50-Ω nominal characteristic impedance.

The finite element method software, CoventorWare, is employed to simulate the behaviors of the RF switch. Figure 3 shows the stress distribution of the switch in the actuated state. The maximum stress, 48 MPa, locates at

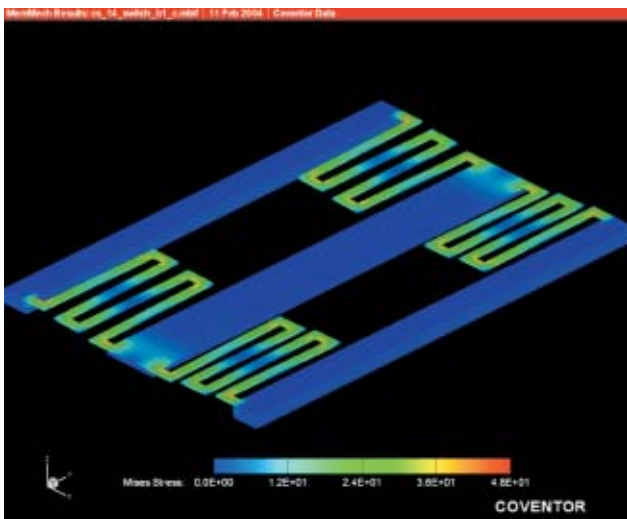


**Figure 3.** The stress distribution of the switch in the actuated state.

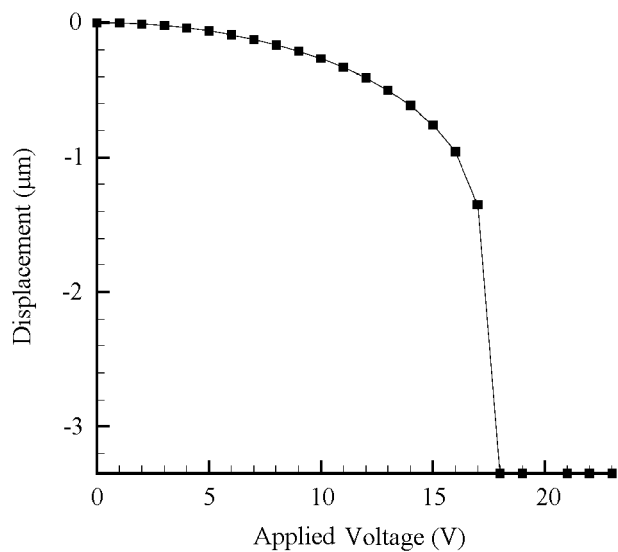


**Figure 4.** Displacement of membrane versus applied voltage.

the corners of the S-shape springs, and the maximum stress value is below the yield strength of aluminum, about 90 MPa. Thus, the deformation of the RF switch can be operated in elastic range. Figure 4 presents the relationship between the applied voltage and the displacement of the membrane. The displacement of the membrane in the switch is about 1 μm at a voltage of 15 V, and the pull-in voltage is approximately 18 V.

### 3. Fabrication of Switch

The RF switch is developed in accordance with the TSMC (Taiwan Semiconductor manufacture Company)

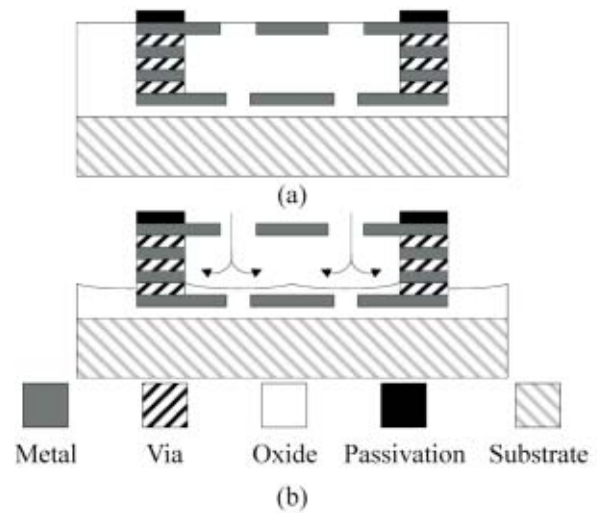


**Figure 5.** Process flow of RF switch: (a) after completed the CMOS process; (b) after the post-process.

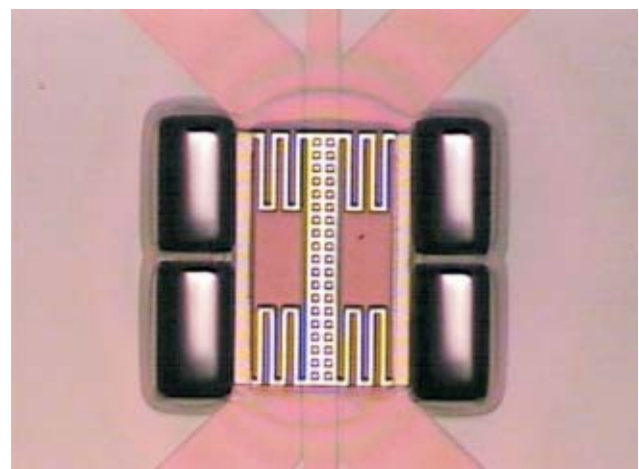


**Figure 6.** Photograph of RF switch after completed the CMOS process.

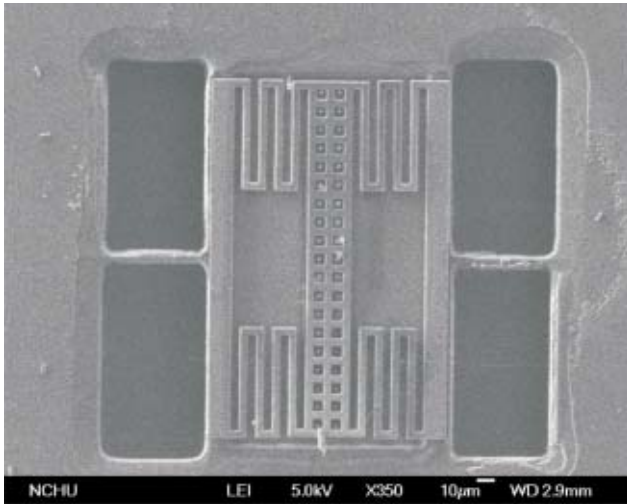


**Figure 7.** SEM photograph of the switch after the post-process.

CMOS foundry service and design rule. The post-process requires only one wet etching with maskless. Figure 5 shows the process flow of the micromachined RF switch. Figure 6 presents the photograph of the RF switch after the TSMC completed the CMOS process. Figure 5(a) illustrates the schematic cross-section view of the RF switch after TSMC completed the CMOS process. Parts of the passivation nitride on the chip were removed in advance, and the top metal layer was exposed. The oxides layer under the membrane and springs are the sacrificial layers. Figure 5(b) depicts the use of wet etching with silox vapox III etchant (ammonium fluoride, glacial acetic acid, aluminum corrosion inhibitor, surfactant and DI water) to etch the sacrificial layers and release the suspended membrane and springs. The etch rate of the etchant for oxide layers was about 4000 Å/minute at room temperature. The etchant has a high etching selectivity for oxide and aluminum metal. Figure 7 demonstrates the SEM (scanning electron microscope) photograph of the RF switch after the post-process.

### 4. Results

A HP8510C network analyzer and a Cascade probe station were used to measure the S-parameters of the RF switch. The S-parameters at microwave frequency stand for transmission and reflection coefficients. The transmission coefficients (S12 and S21) are commonly called

gain or attenuation, and the reflection coefficients (S11 and S22) are directly related to impedance. When without an applied voltage, there is no electrostatic force, and the membrane of the RF switch stays in the up position. The membrane does not couple to microwave propagation in CPW. The RF switch is in the unactuated

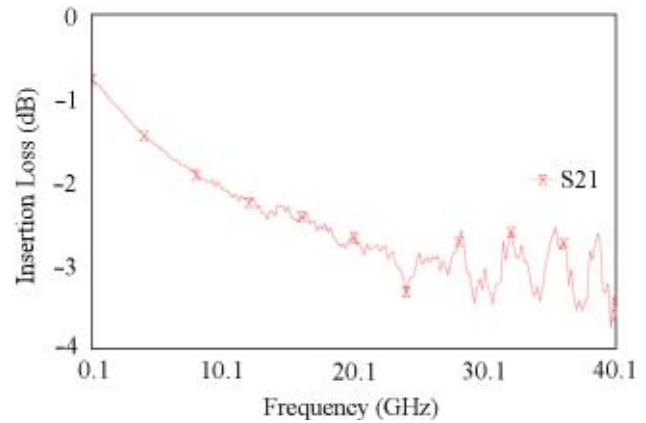


**Figure 8.** Insertion loss.

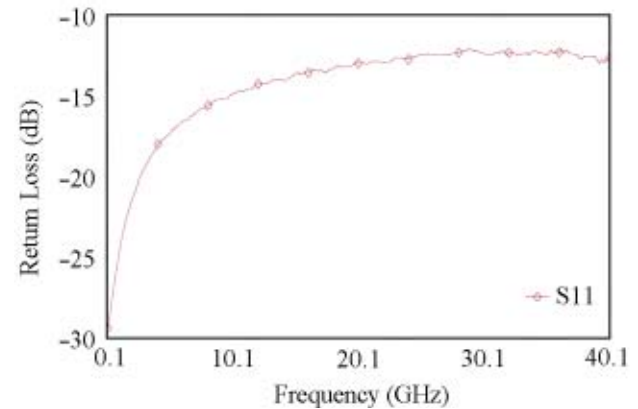


**Figure 9.** Return loss.

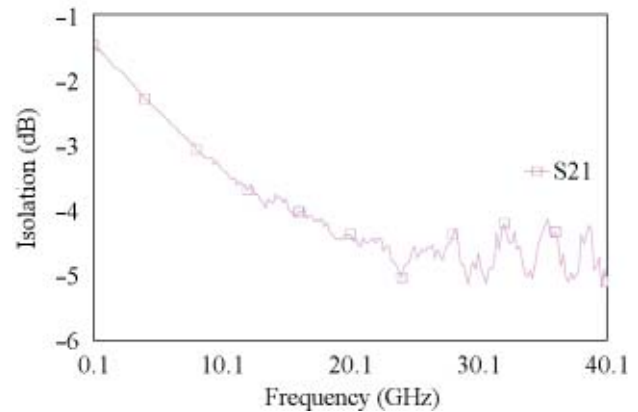


**Figure 10.** Isolation.

state or 'on' state. The S-parameters (S21 and S11) were taken in the range 0–40 GHz using the HP8510C network analyzer and Cascade probe station. The insertion loss (S21) of the RF switch in the unactuated state was  $-2.5$  dB in the range of 10 to 40 GHz, as presented in Figure 8. The return loss (S11) of the RF switch in unactuated state was  $-13$  dB in the range of 10 to 40 GHz, as shown in Figure 9. With an applied voltage, 17 V are applied to the RF switch to make the membrane contact with the signal line of the CPW, so the capacitance coupling intercepts microwave propagation. The RF switch is in the actuated state or 'off' state. The S-parameter (S21) was also taken in the range 0–40 GHz using the HP8510C network analyzer and Cascade probe station. The isolation (S21) of the RF switch in the actuated state was  $-4.5$  dB in the range of 10 to 40 GHz, as shown in Figure 10.

Experimental results show that the pull-in voltage of the RF switch only requires a low voltage of 17 V, and the value is similar to the simulation result (18 V). The RF switch has two merits. One is only needed a simple post-process. The post-process is completed with maskless wet etching. The other is the fabrication of the RF switch compatible with the CMOS process. Thus, the RF switch has a monolithic integration capability with RF circuits as a system on chip (SOC).

## 5. Conclusion

The paper presented the fabrication of the micro-machined RF switch by a fully compatible CMOS process. The post-process was completed with maskless wet etching. Experimental results showed that an insertion loss of  $-2.5$  dB and a return loss of  $-13$  dB in the range 10–40 GHz have been achieved. The pull-in voltage of the RF switch in the actuated state was 17 V. An isolation of  $-4.5$  dB in the range 10–40 GHz was measured. However, The switch proposed herein has a monolithic integration capability with RF circuits.

## Acknowledgement

The authors would like to thank National Center for

High-performance Computing (NCHC) for chip simulation, National Chip Implementation Center (CIC) for chip fabrication and the National Science Council of the Republic of China for financially supporting this research under Contract No NSC 92-2212-E-005-007.

## References

- [1] Yao, J. J., "RF MEMS from a Device Perspective," *J. Micromech. Microeng.*, Vol. 10, pp. R9–R38 (2000).
- [2] Goldsmith, C., Randall, J., Eshelman, S., Lin, T. H., Denniston, D., Chen, S. and Norvell, B., "Characteristics of Micromachined Switches at Microwave Frequencies," *Microwave Symposium Digest, IEEE MTT-S International*, Vol. 2, pp. 1141–1144 (1996).
- [3] Petersen, K. E., "Micromechanical Membrane Switches on Silicon," *IBM J. Res. Develop.*, Vol. 23, pp. 376–385 (1979).
- [4] Goldsmith, C. L., Yao, Z., Eshelman, S. and Denniston, D., "Performance of Low-loss RF MEMS Capacitive Switches," *Microwave and Guided Wave Letters, IEEE*, Vol. 8, pp.269–271 (1998).
- [5] Park, J. Y., Kim, G. H., Chung, K. W. and Bu, J. U., "Monolithically Integrated Micromachined RF MEMS Capacitive Switches," *Sensors and Actuators A: Physical*, Vol. 89, pp. 88–94 (2001).
- [6] Peroulis, D., Pacheco, S. P., Sarabandi, K. and Katehi, L. P. B., "Electromechanical Considerations in Developing Low-voltage RF MEMS Switches," *IEEE Trans. Microwave Theory Tech.*, Vol. 51, pp. 259–270 (2003).
- [7] Shen, S. C., Caruth, D. and Feng, M., "Broadband low Actuation Voltage RF MEM Switches," *Gallium Arsenide Integrated Circuit (GaAs IC) Symposium, 22nd Annual*, pp. 161–164 (2000).
- [8] Mihailovich, R. E., Kim, M., Hacker, J. B., Sovero, E. A., Studer, J., Higgins, J. A. and DeNatale, J. F., "MEM Relay for Reconfigurable RF Circuits," *Microwave and Wireless Components Letters, IEEE*, Vol. 11, pp. 53–55 (2001).
- [9] Milanovi'c, V., Gaitan, M., Bowen, E. D., and Zaghloul, M. Z., "Micromachined Microwave Transmission Lines in CMOS Technology," *IEEE Trans. Microwave The-*

*ory Tech.*, Vol. 45, pp. 630–635 (1997).

- [10] Dai, C. L., Xiao, F. Y., Juang, Y. Z. and Chiu, C. F., “An Approach to Fabricating Microstructures That Incorporate Circuits Using a post-CMOS Process,” *J. Micro-*

*mech. and Microeng.*, Vol. 15, pp. 98–103 (2005).

***Manuscript Received: Feb. 1, 2005***

***Accepted: Apr. 15, 2005***